

Copyright  
by  
Qinhao Xing  
2019

**The Report Committee for Qin hao Xing  
Certifies that this is the approved version of the following Report:**

**The Impact of Different Descriptions on Governor Response in the  
Co-Optimization Model to Provide Primary Frequency Reserve  
in Day-ahead Market**

**APPROVED BY  
SUPERVISING COMMITTEE:**

---

Ross Baldick, Supervisor

---

Surya Santoso

**The Impact of Different Descriptions on Governor Response in the  
Co-Optimization Model to Provide Primary Frequency Reserve  
in Day-ahead Market**

**by**

**Qinhao Xing**

**Report**

Presented to the Faculty of the Graduate School of

The University of Texas at Austin

in Partial Fulfillment

of the Requirements

for the Degree of

**MASTER OF SCIENCE IN ENGINEERING**

**The University of Texas at Austin**

**May 2019**

## **Dedication**

The work is dedicated to my parents, Congli An and Jianhui Xing, who love me, believe in me, inspire me and have supported me every step of the way. The work is also dedicated to my love Jingwei Zhang, who has been accompanying with me in the past eight months.

## **Acknowledgements**

First of all, I wish to thank Dr. Ross Baldick, my supervisor, for introducing me to the wonderful academic topics related to electricity market scheduling and optimization, continually guiding me and giving me confidence and knowledge on this road, and offering me many chances for finding jobs. I would also like to thank Dr. Surya Santoso.

Special thanks to Dr. Cong Liu and Dr. Pengwei Du from ERCOT, for the assistance in arranging relevant research, as well as the patience for answering questions during the research.

Thanks to PhD candidates Manual Garcia and Bing Huang from The University of Texas at Austin, who illuminate the darkness of the current study with their special intelligence.

## **Abstract**

# **The Impact of Different Descriptions on Governor Response in the Co-Optimization Model to Provide Primary Frequency Reserve in Day-ahead Market**

Qinhao Xing

The University of Texas at Austin, 2019

Supervisor: Ross Baldick

With rapid expansion in renewable generation resources (RGS), maintaining system frequency is becoming more significant since conventional generation units have been being substituted by RGS. Therefore, the available primary frequency reserve (PFR) from thermal generators has been reducing, which may even be inadequate under low system inertia conditions. Battery storage and load resources (LR) equipped with under frequency relays can participate in frequency response as fast frequency reserve (FFR). In this report, a co-optimization model in the literature, considering the coordination of PFR and FFR as reserve providers to meet the requirement on frequency response, is introduced, which optimizes the dispatch of generation and reserve simultaneously and reaches maximum social welfare. Moreover, the formulation is modified to represent PFR in terms of system inertia level and headroom (HR) of generation units. Then, four different formulations are proposed and tested with the same case study. Comparisons are

made of the dispatch results of PFR and FFR, as well as the cleared prices of PFR and FFR. Finally, further discussions are presented considering the contribution of different types of frequency response, as well as suggestions for future market policies.

## Table of Contents

List of Tables .....	ix
List of Figures .....	x
Chapter 1. Nomenclature .....	1
Chapter 2. Introduction.....	5
Chapter 3. Reserve Requirement .....	8
Chapter 4. Co-optimization Model.....	14
Chapter 5. Primary Frequency Control Dynamics .....	22
5.1 Governor Model.....	22
5.2 Headroom.....	24
Chapter 6. Formulation of available PFR.....	26
6.1 Constraints Considering Available PFR.....	27
Chapter 7. Case Study .....	31
7.1 Case Introduction.....	31
7.2 Scenario Description.....	33
7.3 Objective Function Value .....	35
7.4 Dispatch Results Analysis .....	38
7.5 Cleared Prices Comparison.....	42
Chapter 8. Conclusion .....	49
Chapter 9. Future Work.....	50
Bibliography .....	52

## **List of Tables**

Table 1: Minimum FFR Requirement, Equivalency Ratios, Product of Inertia and Equivalency Ratio, and FFR Requirement Intercept [6] (Source: Based on Table II) .....	12
Table 2: Bidding Parameters and Capacities of Load Resources [7] (Source: Table II).....	32
Table 3: Capacity Percentages of Load Resources [7] (Source: Table III) .....	33
Table 4: Total High Sustainable Limits of Low Penetration of Wind Generation [7] (Source: Table IV) .....	34
Table 5: Total High Sustainable Limits of High Penetration of Wind Generation [7] (Source: Table V).....	34
Table 6: Objective Value .....	35
Table 7: Computational Gap.....	37

## List of Figures

Figure 1: Dynamic Simulation Criteria (Source: Figure 3 of [6]) .....	11
Figure 2: Combination of PFR and FFR for meeting minimum FFR requirement (Source: Figure 4 of [6]) .....	11
Figure 3: Inertia Constant with Different Units [7] (Source: Figure 4) .....	16
Figure 4: Ratio-Inertia Curve (Source: Figure 2 of [7]) .....	18
Figure 5: FFR requirement-Inertia Curve (Figure 3 of [7]) .....	19
Figure 6: Governor Model [12] (Source: Figure 1) .....	23
Figure 7: IEEE 118 Bus System Diagram .....	32
Figure 8: PFR Dispatch Result Comparison: ERMM.....	39
Figure 9: FFR Dispatch Result Comparison: ERMM.....	39
Figure 10: PFR Dispatch Result Comparison: DMM.....	40
Figure 11: FFR Dispatch Result Comparison: DMM.....	41
Figure 12: PFR Dispatch Result Comparison: DDMM.....	42
Figure 13: FFR Dispatch Result Comparison: DDMM.....	42
Figure 14: Cleared price comparison for PFR: ERMM.....	43
Figure 15: Cleared price comparison for FFR: ERMM.....	44
Figure 16: Cleared price comparison for PFR: DMM.....	45
Figure 17: Cleared price comparison for FFR: DMM.....	45
Figure 18: Cleared price comparison for PFR: DDMM.....	47
Figure 19: Cleared price comparison for FFR: DDMM.....	47

## Chapter 1. Nomenclature

### Indexes:

$i$	Index of generation units
$j$	Index of loads
$t$	Index of time periods
$s$	Index of segments
$q$	Index of segments in start-up curves
$l$	Index of transmission branches

### Variables:

$P$	Cleared energy
$L$	Cleared demand
$I, Y, Z$	Binary indicators for unit on/off, start-up and shutdown
$\delta$	Binary variables indicating a segment in a linearized curve is activated
$STC$	Start-up cost of a generating unit
$RUP$	Regulation up reserve of generation units
$RDN$	Regulation down reserve of generation units
$NSR$	Non-spinning reserve of generation units
$PFR$	Cleared frequency response reserve from primary frequency response of generating units
$FFR$	Cleared frequency response reserve from fast frequency response of loads
$FRR$	Total cleared frequency response reserve
$RUPN$	Not served regulation up reserve
$RDNN$	Not served regulation down reserve

$FRRN$	Not served frequency response reserve
$NSRN$	Not served non-spinning reserve
$PFRN$	Not served primary frequency response reserve
$Inx$	Inertia value of a segment in a linearized curve
$\beta$	Variable to replace bilinear terms
$\lambda, \theta, \gamma, \rho, \tau, \pi, \sigma$	Shadow prices

**Functions:**

$\alpha$	Equivalent Ratio between FFR and PFR, depending on the total inertias of committed generation units
$Rfrr$	Total requirement of frequency response reserve, depending on the total inertias of committed generation units
$Ce$	Energy cost/benefit curve based on energy offers/bids

**Constant and Sets:**

$G$	Sets of generation units
$D$	Sets of demands
$T$	Sets of time periods
$B$	Sets of transmission branches
$N$	Sets of segments
$Csu$	Step constant in the start-up cost curve of generation units
$Cf$	Minimum energy price
$Cr_{dn}, Cr_{up}$	Offer price for regulation up and down reserve from generating units
$C_{pfr}$	Offer price for fast frequency response from loads and non-spinning reserve from generating units
$Nr_{up}, Nr_{dn}$	Penalty price for unserved regulation up and down

$N_{frr}, N_{nsr}$	Penalty price for unserved frequency responsive reserve and non-spinning reserve
$N_{pfr}$	Penalty price for unserved primary frequency response reserve from generation units
$R_{rup}, R_{rdn}$	Total requirement of regulation up/down reserve
$R_{nsr}$	Total requirement of frequency responsive reserve and non-spinning reserve
$R_{pfr}$	Total requirement primary frequency response reserve from generating units
$LSL, HSL$	Low and high sustainable limits of generating units
$MPC$	Maximum power consumption for a demand
$MT_{on}, MT_{off}$	Minimum on/off time of generating units
$RU, RD$	Maximal ramp up/down limits per hour of generating units
$QSC$	Quick start capacity of generating units in 30 minutes
$H$	Inertial constant
$S$	Rated power of generating units
$SF$	Generator/load shift factor of power network
$\overline{PL}$	Capacity limit of a transmission branch
$\overline{RUP}, \overline{RDN}, \overline{PFR}$	Upper bounds of available regulation up/down reserves and PFR of generating units
$Ratio$	The step value of the Ratio-Inertia curve
$RFRR$	The point value in vertical scale of the FRR requirement-Inertia curve
$In$	The inertia value of the linearized curves
$M$	A larger positive number

**Added Indexes, Variables and Constants:**

$\omega$	Variables to replace bilinear terms
$N$	A larger positive number
$sPFR$	Separated segment of PFR
$k$	Index of generation units

## Chapter 2. Introduction

During late of 19th century, there was a doubt about the choice of commercial electricity. One of the candidates is direct current (DC) with unidirectional flow of current. However, the alternating current (AC) with periodically reversing current direction was chosen since it takes the advantage of lower cost in transmission and distribution in power system although AC present other problems. One of these problems is system frequency. If system frequency varies abnormally from its nominal value of 50 Hz or 60 Hz, electrical equipment may operate abnormally, leading to potential damages.

It is critical to maintain the system frequency within a target range. As discussed in [1] and [2], the exact roles of primary, secondary, and tertiary control vary across different systems. In North America, primary frequency control usually refers to decentralized proportional control of generation output based on locally measured frequency at each generator using the "governor." In the particular case of the Electric Reliability Council of Texas (ERCOT), all generators that are not at maximum or minimum output are required to provide governor response. Secondary control typically uses proportional plus integral control commanded from a centralized control center. In the particular case of ERCOT, secondary control does not have an integral term, but the feedback equation is nonlinear from frequency to commanded generation. Tertiary control refers to the automatic or manual change in the operating points of online generation units. In ERCOT, it is predominantly accomplished automatically through the

operation of the real-time market, which updates generator operating points every 5 minutes, or more often in the event of a contingency.

Among the three levels of frequency control, the primary frequency control (PFC) is more vulnerable to changes resulting from increasing amounts of renewable production, since a significant number of synchronous generators are being replaced by renewable power resources, including wind farms and solar panels, and less amount of thermal generation units are available to provide PFC. More importantly, increasing introduction of renewable generation declines the system inertia level. It is the kinetic energy stored in inertia that responds first to the generation-demand imbalance, which causes frequency drop with PFC then further opposing the imbalance. With the decline in system inertia level, the frequency drop rate increases, thus reducing the ability of PFC to respond in a timely fashion. This is becoming a significant issue in power grids in North America, Australia and Ireland.

The existing North American electricity markets include reserve trading and ancillary service provision from generation resources in order to provide secondary reserves. Historically, in North America, most or all generation has been required to provide primary frequency reserves when not operating at maximum or minimum. However, more and more primary reserves are needed to maintain primary frequency reserve (PFC) in the lower-inertia situation.

As a result of this trend, other resources are needed to fulfill the requirement on frequency response reserve (FRR) in order to provide PFC during large contingencies.

Novel solutions include so-called fast frequency reserve (FFR) from electronic generation resources, including wind turbines, solar panels, energy storage, and demand response.

Since the system inertia level is declining due to renewable generations penetration, fast-reacting energy sources are increasingly needed to respond quickly and stabilize the frequency variation under the low-inertia environment. However, there is a cost for FFR and coordination of FFR resources with the existing market mechanism is still a problem.

[3] [4] Furthermore, the contribution from PFR and FFR needs to be qualified before designing the market rules for ancillary service.

Therefore, this report mainly focuses on three issues related with frequency reserve. The first is to determine the effectiveness of PFR and FFR in providing PFC. The second issue is to introduce the co-optimization model from [7] that considers both the PFR and FFR simultaneously to maximize the social welfare, along with the relationship between PFR and FFR. The third issue is to discuss an alternative formulation of PFR and modified constraints in the previous co-optimization model from [7] to provide a simplified implementation.

### **Chapter 3. Reserve Requirement**

The Electric Reliability Council of Texas (ERCOT) is an Independent System Operator (ISO) in Texas. In ERCOT, traditional requirement on PFR is set in the BAL-003 standard, which is mainly fulfilled by the contribution from generation units. The frequency obligation for ERCOT is 413MW/0.1Hz [5]. Besides, the droop setting should not exceed 5% and the frequency response dead band should be no more than  $\pm 0.017$  Hz. As for the newly introduced fast frequency reserve (FFR), ERCOT just requires FFR to fully respond within 30 cycles when the frequency drops below certain threshold and has no specific value requirement on it currently.

Frequency Response Reserve (FRR) activates when the frequency changes as kinetic energy is withdrawn or added to the rotating mass in the system to reestablish generation-demand balance. When a contingency happens, the amount of FRR needs to be sufficient to withstand criteria set by ISOs. In ERCOT, the minimum requirement on FRR is determined by “the worst-case scenario”, which refers to a contingency including losses of two largest units equal to 2750 MW. During such a contingency, the system frequency nadir should be arrested before dropping below 59.3 Hz. However, this fixed requirement did not consider the penetration of renewable resources, which lowers the system inertia level by substituting thermal generation units, as discussed in Chapter 2. So the requirement on FRR may change with the variation of system inertia level.

To prepare for a low-inertia environment, the FFR product has been defined in ERCOT to participate in FRR. This requires that some tradeoff be established between PFR and FFR. That is, an equivalency between PFR and FFR needs to be established. In [6], a detailed qualification of FRR minimum requirement as well as the direct linkage coordinating PFR and FFR is established under the guidance of a new approach.

Basically, this approach contains four parts. First, a range of values for the ERCOT system inertia level, ranging from 15 GW to 65 GW, are considered. Totally 12 representative inertia values are selected as the system environments for the dynamic simulation. Second, the dynamic simulations are set up for the scenario where the two largest generation units (2750 MW) are outaged, and the frequency response criterion is that the system frequency should stay within the range of between 59.4 Hz to 60.4 Hz. The acting frequency threshold of FFR is set as 59.7Hz, while the under-frequency threshold is set as 59.3Hz, which is shown in Figure 1. Then, before each dynamic simulation, the amount of PFR is adjusted by adding or removing the governor control, and the amount of FFR is adjusted by connecting or disconnecting the load resources and battery storages under the same system inertia. So the minimum requirement can be identified when the frequency drop nadir reaches 59.4 Hz after losing two of the largest units, which is shown in Figure 1. Finally, all the results are summarized in Table 1, and the equivalency ratio can be obtained from the slopes of the line in Figure 2, where the points represent dynamic simulations within a specific system inertia value.

Based on the description on dynamic simulation above, FRR is provided by both PFR and FFR, which need to fulfill the minimum requirement collectively of maintaining the frequency nadir above 59.3 Hz. (Simulations actually used a minimum of 59.4 Hz to represent a safety margin). So the constraint on FFR should describe the requirement, which is shown as follows,

$$FRR_t = \sum_{i \in G} PFR_{i,t} + \alpha \cdot (\sum_{j \in D} FFR_{j,t}) \geq Rffr_t \quad (1)$$

where  $FRR_t$  is the total provision of FRR during interval  $t$ , being the result of the PFR provided by all the generators  $i \in G$  at time  $t$ , together with a scaled version of the FFR provided by all of the FFR resources  $j \in D$  at time  $t$ . Since the FFR can respond to frequency deviation within 30 cycles, the scaling is due to the fact that 1MW of FFR may be able to contribute more to FRR than 1MW of PFR. Reformation of this constraint will be considered in Chapter 5 and 6. In addition, ERCOT also needs to fulfill the minimum requirement on PFR according to the BAL-003 standard, which is 1150 MW, as

$$\sum_{i \in G} PFR_{i,t} \geq Rpfr_t \quad (2)$$

where the requirement for FRR at time  $t$  is specified by  $Rpfr_t$ . The equivalency ratio,  $\alpha$ , is therefore introduced to represent the effective ratio between PFR and FFR. In other words, it represents the amount of PFR that can be substituted by the unit amount of FFR in frequency response. The equivalency ratio  $\alpha$  can also be gained from the dynamic simulations with varying amounts of PFR and FFR while keeping the total inertia level invariant. The comparison of combinations of PFR and FFR under different system

inertia level is shown in Figure 2, where each point within a single line represents one dynamic simulation under identical system inertia level, and the slope of the lines represents the equivalency ratio  $\alpha$ . The steps and details are included in [6]. The results showing the requirement on FRR for different inertia levels and the corresponding equivalency ratio  $\alpha$  are summarized in Table 1.

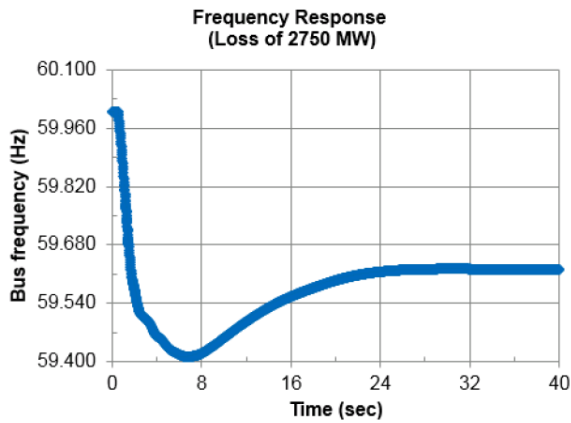


Figure 1: Dynamic Simulation Criteria (Source: Figure 3 of [6])

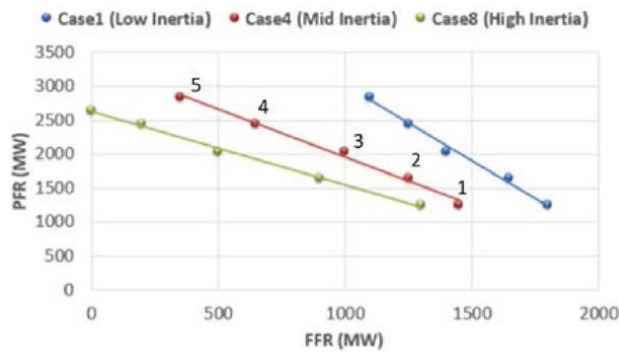


Figure 2: Combination of PFR and FFR for meeting minimum FRR requirement (Source: Figure 4 of [6])

Case No.	Inertia (GW·s)	$Rffr_t$ (MW)	Equivalency Ratio ( $\alpha_t$ )	Product of Inertia and Equivalency Ratio	FFR Requirement
					Intercept
1	120	5200	2.2	264	2363.64
2	136	4700	2.0	272	2350
3	152	3750	1.5	228	2500
4	177	3370	1.4	247.8	2407.14
5	202	3100	1.3	262.6	2384.6
6	230	3040	1.25	287.5	2432
7	256	2640	1.13	289.28	2336.28
8	278	2640	1.08	300.24	2444.44
9	297	2240	1	297	2240
10	316	2280	1	316	2280
11	332	2140	1	332	2140
12	350	2140	1	350	2140

Table 1: Minimum FFR Requirement, Equivalency Ratios, Product of Inertia and Equivalency Ratio, and FFR Requirement Intercept [6] (Source: Based on Table II)

In addition, the results showing the product of inertia and equivalency ratio, as well as the FFR requirement intercept by corresponding equivalency ratio, are listed in Table 1. Note that for cases with equivalency ration greater than 1, the FFR requirement intercepts

are all around the constant number 2400, which is introduced into the reformation of PFR along with the concept of “available PFR” later.

## Chapter 4. Co-optimization Model

Based on the constraints on FFR and PFR discussed above, the day-ahead market establishes a unit commitment model where generation and reserve both participate [7]. The objective function, which is shown in (3) below, is to maximize the total social welfare. It represents the total benefits of consumption minus energy costs from generation, reserve costs from both generation units and load resources and unserved reserve cost, which is the penalty fee. Based on the two modes for unit start in generation unit modeling, hot-start and cold-start, the start-up cost constraint (4) is a function of the turning-on indicator and the number of hours since the generation units have been turned off. If the units have been turned off for a long period of time, the start-up cost would be much higher than the case when the units are turned on within a shorter period.

$$\begin{aligned}
 Max \quad & \sum_{j \in L} \sum_{t \in T} [Ce_{j,t}(L_{j,t}) - Cffr_{j,t} \cdot FFR_{j,t}] \\
 & - \sum_{i \in G} \sum_{t \in T} [STC_{it} + C_f \cdot I_{i,t} + Ce_{i,t}(P_{i,t}) \\
 & \quad + Crup_{i,t} \cdot RUP_{i,t} + Crdn_{i,t} \cdot RDN_{i,t} \\
 & \quad + Cnsr_{i,t} \cdot NSR_{i,t} + Cpfrr_{i,t} \cdot PFR_{i,t} \\
 & - \sum_{t \in T} [Nrup_t \cdot RUPN_t + Nrdn_t \cdot RDNN_t \\
 & \quad + Nnsr_t \cdot NSRN_t + Npfrr_t \cdot PFRN_t \\
 & \quad + Nffrr_t \cdot FRRN_t]
 \end{aligned} \tag{3}$$

s.t.

$$STC_{i,t} \geq CSu_{i,q} \cdot \left[ Y_{i,t} - \sum_{n=1}^{\min(t,q)} I_{i,t-n} \right], STC_{i,t} \geq 0 \quad \forall i \in G, \forall t \in T \quad (4)$$

$$1 - I_{i,t-1} \geq Y_{i,t} \quad \forall i \in G, \forall t \in T \quad (5)$$

$$I_{i,t-1} \geq Z_{i,t} \quad \forall i \in G, \forall t \in T \quad (6)$$

$$I_{i,t} - I_{i,t-1} \geq Y_{i,t} - Z_{i,t} \quad \forall i \in G, \forall t \in T \quad (7)$$

$$0 \leq Y_{i,t}, Z_{i,t} \leq 1 \quad \forall i \in G, \forall t \in T \quad (8)$$

$$I_{i,t} \geq \sum_{\tau=\max\{1,t-MT_{on,i}+1\}}^t Y_{i,\tau} \quad \forall i \in G, \forall t \in T \quad (9)$$

$$1 - I_{i,t} \geq \sum_{\tau=\max\{1,t-MT_{off,i}+1\}}^t Z_{i,\tau} \quad \forall i \in G, \forall t \in T \quad (10)$$

$$-RD_i \leq P_{i,t} - P_{i,t-1} \leq RU_i \quad \forall i \in G, \forall t \in T \quad (11)$$

$$P_{i,t} + RUP_{i,t} + PFR_{i,t} \leq HSL_i \cdot I_{i,t} \quad \forall i \in G, \forall t \in T \quad (12)$$

$$P_{i,t} - RDN_{i,t} \geq LSL_i \cdot I_{i,t} \quad \forall i \in G, \forall t \in T \quad (13)$$

$$0 \leq RUP_{i,t} \leq \overline{RUP}_i \cdot I_{i,t} \quad \forall i \in G, \forall t \in T \quad (14)$$

$$0 \leq RDN_{i,t} \leq \overline{RDN}_i \cdot I_{i,t} \quad \forall i \in G, \forall t \in T \quad (15)$$

$$0 \leq PFR_{i,t} \leq \overline{PFR}_i \cdot I_{i,t} \quad \forall i \in G, \forall t \in T \quad (16)$$

$$0 \leq NSR_{i,t} \leq QSC_i \cdot (1 - I_{i,t}) \quad \forall i \in G, \forall t \in T \quad (17)$$

$$0 \leq FFR_{j,t} \leq L_{j,t} \leq MPC_{j,t} \quad \forall i \in G, \forall t \in T \quad (18)$$

$$\sum_{i \in G} P_{i,t} = \sum_{j \in L} L_{d,t} \quad \forall i \in G, \forall t \in T \quad (19)$$

$$-\overline{PL}_l \leq \sum_{i \in G} SF_{l,i} P_{i,t} + \sum_{j \in L} SF_{l,j} L_{j,t} \leq \overline{PL}_l \quad \forall i \in G, \forall t \in T \quad (20)$$

$$RUPN_t, RDNN_t, NSRN_t, NPFR_t, FRRN_t \geq 0 \quad \forall t \in T \quad (21)$$

$$RUPN_t + \sum_{i \in G} RUP_{i,t} \geq Rrup_t \quad \forall t \in T \quad (22)$$

$$RDNN_t + \sum_{i \in G} RDN_{i,t} \geq Rrdn_t \quad \forall t \in T \quad (23)$$

$$NSRN_t + \sum_{i \in G} NSR_{i,t} \geq Rnsr_t \quad \forall t \in T \quad (24)$$

$$PFRN_t + \sum_{i \in G} PFR_{i,t} \geq Rpfr_t \quad \forall t \in T \quad (25)$$

$$FRRN_t + FRR_t \geq Rfrr_t (\sum_{i \in G} I_{i,t} \cdot H_i \cdot S_i) \quad \forall t \in T \quad (26)$$

$$FRR_t = \sum_{i \in G} PFR_{i,t} + \alpha_t (\sum_{i \in G} I_{i,t} \cdot H_i \cdot S_i) \cdot (\sum_{j \in L} FFR_{j,t}) \quad \forall t \in T \quad (27)$$

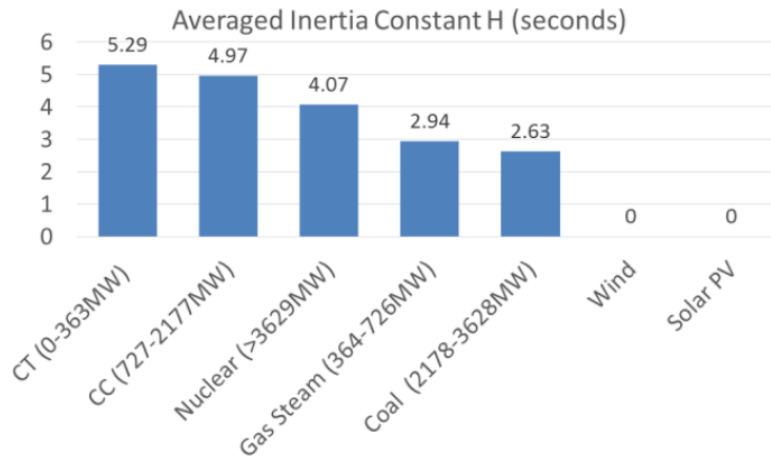


Figure 3: Inertia Constant with Different Units [7] (Source: Figure 4)

Constraints (5)-(8) represents the coupling relationships of unit commitment status with three vectors of binary variables  $I$ ,  $Y$ ,  $Z$ . Binary variable  $I$  represents the on/off indicator for the generation units, while  $Y$  and  $Z$  are the start-up indicator and shut-down indicator, respectively. Constraints (9) and (10) state the minimum on/off time limits on each generation unit, which means a generation unit must stay on or off for the required period of time if it is turned on or turned off. Constraint (11) shows the ramp rate of each

generation unit from period to period. Constraints (12)-(16) define the limits and bounds on generation and reserve provided by generation units, as well as their coupling relationships. Constraint (17) emphasizes that non-spinning reserve (NSR) should be provided by offline units which can start up within 30 minutes. (In practice, online units can also provide NSR) Constraint (18) shows the limits on FFR from the load resources, as well as the bounds on load variation. (In principle, the formulation could be expanded to include FFR from battery resources as well)

Constraint (19) represents the power balance constraint. Constraint (20) represents the transmission line capacity constraint, where the  $SF$  in (20) is the shift factor matrix, representing the flow change due to a unit amount of power injection from a particular bus [8]. Constraint (21)-(24) states the minimum requirements on three types of reserves, including regulation up/down and non-spinning reserve based on the existing criteria in ERCOT.  $RUPN_t, RDNN_t, NSRN_t, NPFR_t, FRRN_t$  represent the amounts of unserved reserves. The unserved reserve holds an extremely high penalty price in the objective function, so the unserved reserve would tend to be zero value under normal conditions. (In practice, ERCOT uses an “Operating Reserve Demand Curve” to set prices for unserved reserves.) Constraint (25) denotes the minimum requirement on PFR discussed previously. Constraint (26) and (27) show the requirement on frequency response reserve and the composition of FFR as shown above. Based on the results of dynamic simulation in Table 1, the minimum requirement on FFR and equivalency ratio  $\alpha$  are all functions of system inertia level, which is contributed by committed generation units and is defined as

the sum of the multiplication of inertia constant and the rated power from the committed generation units. The rated power is determined by the highest sustainable limit of the generation unit, while the inertia constant is determined by the type of generator, as shown in Figure 3.

However, there is still one concern about the formulation in the co-optimization above. The FRR requirement-Inertia and Ratio-Inertia relationships shown in constraint (26) and (27) are based on dynamic simulation results, which are 12 individual cases, and thus the two relationships are non-linear. In addition, constraint (27) also contains the product of the binary variable and the continuous variable, which cannot be solved by mixed-integer solver. The two relationships mentioned above need to be linearized and the product in constraint (27) also needs to be transformed with big M method.

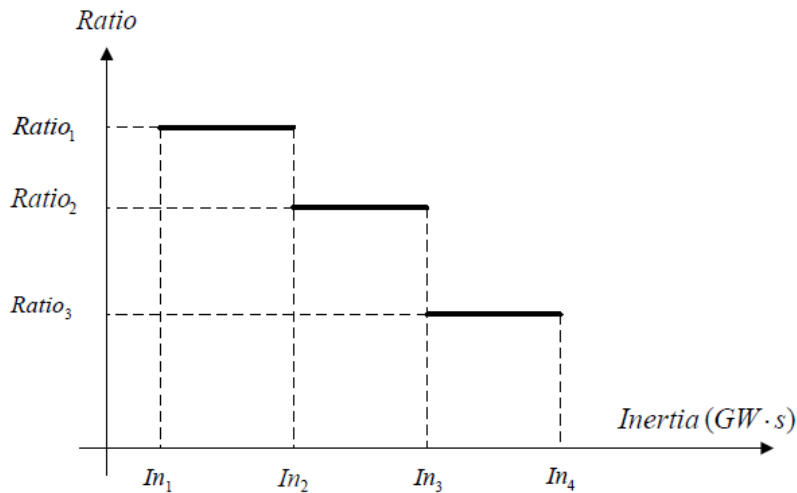


Figure 4: Ratio-Inertia Curve (Source: Figure 2 of [7])

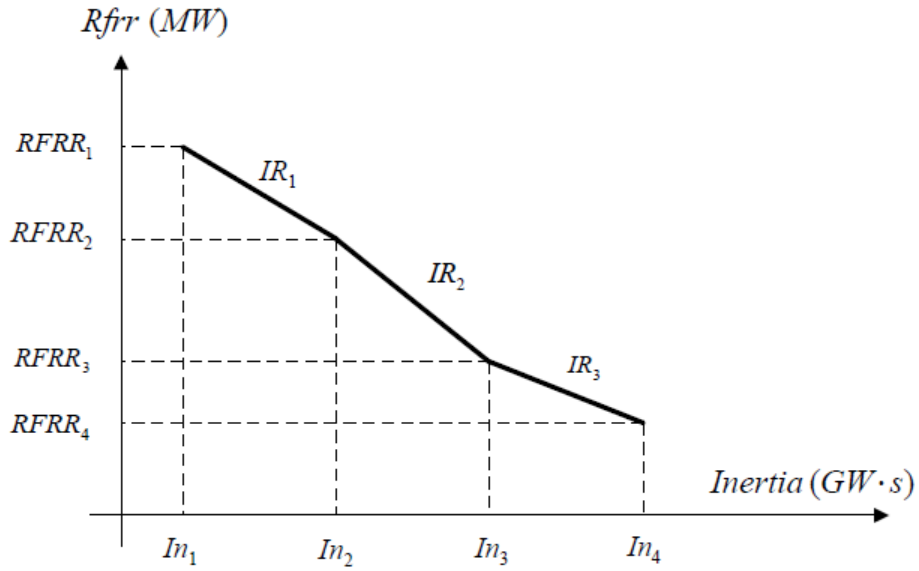


Figure 5: FRR requirement-Inertia Curve (Figure 3 of [7])

In order to solve the two problems mentioned above, constraint (26) and (27) are reformulated in [7] as (28)-(34). For the linearizations on the FRR requirement-Inertia and Ratio-Inertia relationships, an additional vector of binary variables  $\delta$  is introduced into the model to represent activation of the segment in the piece-wise linear curves representing the two relationships, as shown in Figure 4 and Figure 5. It is clear that the piece-wise curve is divided into several segments on the horizontal axis, and the value for each segment can also vary within its limit, which is represented by the continuous variable  $Inx$ . Therefore the value of vertical axis can be obtained as a function of  $\delta$  and  $Inx$ . Constraint (31) shows that the current segment must be activated if next segment is activated. Constraint (32) defines the upper and lower bounds of each segment. If the next segment is activated, the current segment must be binding to the maximum value. If

the next segment is not activated, the current segment must be zero. Constraint (29) states that the total system inertia level equals the sum of the inertia contribution from all committed generation units. Constraint (28) shows the minimum requirement on FRR, where IR is the slope of the piece-wise linear curve of Figure 5.

$$FRRN_t + FRR_t \geq RFRR_1 + \sum_{s \in N} IR_s \cdot Inx_{i,t} \quad \forall t \in T \quad (28)$$

$$In_1 + \sum_{s \in N} Inx_{s,t} = \sum_{i \in G} I_{i,t} \cdot H_i \cdot S_i \quad \forall t \in T \quad (29)$$

$$(In_{s+1} - In_s) \cdot \delta_{s+1,t} \leq Inx_{s,t} \leq (In_{s+1} - In_s) \cdot \delta_{s,t} \quad \forall s \in N, \forall t \in T \quad (30)$$

$$\delta_{s+1,t} \leq \delta_{s,t} \quad \forall s \in N, \forall t \in T \quad (31)$$

$$FRR_t = \sum_{i \in G} PFR_{i,t} + \beta_t \quad \forall t \in T \quad (32)$$

$$\beta_t \geq Ratio_s \cdot \sum_{j \in D} FFR_{j,t} - M_{s,t} \cdot (1 - \delta_{s,t} + \delta_{s+1,t}) \quad \forall s \in N, \forall t \in T \quad (33)$$

$$\beta_t \leq Ratio_s \cdot \sum_{j \in D} FFR_{j,t} + M_{s,t} \cdot (1 - \delta_{s,t} + \delta_{s+1,t}) \quad \forall s \in N, \forall t \in T \quad (34)$$

In order to solve the problem considering the product of binary variable and continuous variable, the big M method is introduced into the model to relax the feasible region, which is constraints (32)-(34). If the difference between  $\alpha_{s,t}$  and  $\alpha_{s,t+1}$  equals zero, the constraints (33) and (34) are relaxed due to the large value of constant  $M$ . If the difference is one,  $\beta_{s,t}$  is set equal to the constant value  $Ratio_s \cdot \sum_{j \in D} FFR_{j,t}$ . Therefore the product is separated as the three constraints [9]. Note that the choice of value on  $M$  should be large enough to ensure the relaxation of the two constraints when the difference between  $\alpha_{s,t}$  and  $\alpha_{s,t+1}$  equals zero. However, in order to minimize the computational effort, it is worth to discuss the maximum possible value of  $\beta_{s,t}$ , which is a perfect

choice for the value of  $M$ . Since the maximum possible value of  $Ratio_s \cdot \sum_{j \in D} FFR_{j,t}$  is  $Ratio_s \cdot \sum_{j \in D} MPC_{j,t}$  according to the constraint (18), this sets the upper bound on FFR. It is therefore sufficient to choose  $M_{s,t} = Ratio_s \cdot \sum_{j \in D} FFR_{j,t}$ . Choosing the smallest value of  $M$  sufficient with the upper bound makes the model tighter, and therefore solve faster.

## Chapter 5. Primary Frequency Control Dynamics

This chapter describes two concepts relating to primary frequency control dynamics. The governor model will be discussed in Section 5.1, while headroom will be discussed in Section 5.2. These concepts will be used in the reformulation of the frequency response reserve constraint in Chapter 6.

### 5.1 GOVERNOR MODEL

The co-optimization model described above holds much potential in ERCOT, where the renewable generation resources grow rapidly recently. However, the constraints on different types of reserve just consider the capacity limits on generation units, and ignore the response speed. While FFR from load resources can act fast within 30 cycles, PFR needs a few seconds to respond to frequency drop. Based on the considerations, frequency response dynamic is given as swing equation (35) [10]:

$$\frac{df(t)}{dt} = \frac{1}{M_H} (P_m(t) - P_e(t)) \quad (35)$$

where  $f(t)$  is the system frequency in Hz,  $P_m(t)$  is the system mechanical power in MW,  $P_e(t)$  is system electrical load in MW, and  $M_H$  is the system inertia in MWs.

During normal operations, the generation and demand reach a balance, and the difference between  $P_m(t)$  and  $P_e(t)$  is quite small. If the sudden contingency occurs, the difference between  $P_m(t)$  and  $P_e(t)$  becomes significant, frequency starts declining, and governors respond by increasing mechanical power to re-establish the balance between  $P_m(t)$  and  $P_e(t)$ , as shown in Figure 6.

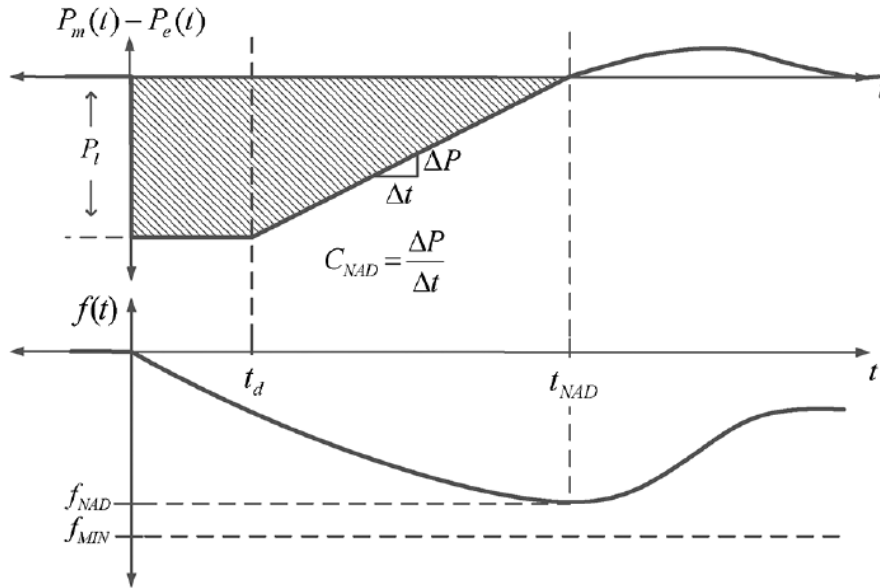


Figure 6: Governor Model [12] (Source: Figure 1)

The governor refers to the controller for a generator and will be modeled based on Figure 6, where it is assumed that the governor starts operating at a dead-band time  $t_d$  and then power increases linearly with slope  $c_{NAD}$  thereafter. It is used to measure and regulate the speed of generator by controlling the valves of the generator turbine to oppose changes in system frequency. Primary frequency control from the governor is also called droop control. The dynamics of the governor model can be found in detail in the block diagram in [11], and the feedback control loops there offer a clear view of potential outputs for different situations. To simplify the case of a sudden contingency, a single constraint on governor ramping capability has been modeled in [12]. This model considers the overall power response to the loss of generation  $P_l(t)$  MW, assuming a constant ramp rate  $c_{NAD}$ . Although in reality the frequency response is not a constant

value, the ramp rate is a good approximation that facilitates the analysis. Equation (35) can also be transformed to (36) with the integration on both sides from  $t = 0$  to  $t = t_{NAD}$ , as shown below:

$$\int_0^{t_{NAD}} \frac{df(t)}{dt} dt = f(t_{NAD}) - f(0) = f_{NAD} - f_0 = \frac{1}{M_H} \int_0^{t_{NAD}} (P_m(t) - P_e(t)) dt \quad (36)$$

where the  $f(0)$  is the initial frequency, and  $t_{NAD}$  is the time when system frequency reaches its nadir. With further calculation, (36) can be rewritten as:

$$f_{NAD} - f_0 = \frac{1}{M_H} \int_0^{t_d} -P_l(t) + \frac{1}{M_H} \int_0^{t_{NAD}-t_d} C_{NAD}t - P_l dt \quad (37)$$

where the  $t_d$  is the governor dead-band time, which represents the time delay after a contingency until the governor acts.

Equation (37) divides the integral into two parts before and after time  $t_d$ , which are represented as the two shaded regions in Figure 6, which are easy to calculate as:

$$f_{NAD} - f_0 = -\frac{1}{M_H} \left( P_l t_d + \frac{P_l^2}{2C_{NAD}} \right) \quad (38)$$

From (38), the frequency drop to the nadir can be written as a function of system inertia, and the ramp rate, when the loss of generation and dead-band time are given. Based on this model, we consider a reformulation on the frequency reserve provided by generation units as discussed in the next chapter.

## 5.2 HEADROOM

Headroom (HR) refers to the online capacity that is ready to be dispatched. It is, in principle, available to provide sufficient amount of reserve to cover the deviation of real-

time net load and forecast load value. With increasing penetration of renewable resources, including wind power and solar energy, headroom of dispatched generation units tends to be increased in day-ahead unit commitment to provide enough reserve. Consequently, generation units may be required to not operate at economically optimal points [13].

Inertia in power system refers to the rotating mass that stores kinetic energy. The rotational speed of a synchronous generator or motor is proportional to the electricity frequency in system. When a sudden loss of generation happens, there is an imbalance between mechanical and load power, and generators and motors tend to transfer kinetic energy into electrical power, which lowers the rotational speed and, therefore, is associated with a frequency drop.

## Chapter 6. Formulation of available PFR

According to research from ERCOT [7], the required amount of PFR is set to be sufficient to fulfill both the PFR requirement based on BAL-003 standard, and the requirement on total reserve including PFR and FFR. Moreover, the capacity of a single generator to provide PFR is also defined as a fixed value. However, such assumptions might not be satisfied. That is because generators usually won't set bounds for capacity provided as PFR, and PFR can be obtained from all the remaining capacity of generation units, which is called the headroom. Besides, although the dynamic simulation considers the reliability criterion, PFR provided from generation units may not be fully dispatched before frequency drop passes the threshold for the under-frequency load shedding (UFLS), which corresponds to "the worst-case scenario". In order to better describe the available primary frequency response, a reformulation of PFR is proposed, namely "available PFR", which considers the perspective of primary frequency control dynamics discussed in Chapter 5.

When developing constraints on the performance of the governor, a simpler linear description can be introduced on governor ramp capability. This model represents the governor response of generator units to loss of generation as having a constant ramp rate  $c_{NAD}$ . Limits on reserve from primary frequency control are also set based on generator ramp rate and system inertia level. Although the ramp rate of the governor is not exactly a constant value, linearization of governor response curve allows for a simplified analysis that may be adequate to characterize sufficient PFR.

However, it is worth to notice that, governor ramp rate  $c_{NAD}$  can only be obtained from a stress test [12], which might contain risks. One of the risks is that the stress test

requires the protection system operating at abnormal states and many over-speed incidents occurs during stress tests. Besides, with increasing generation capacity introduced into power system, the amount of stress tests may also increase when new types of units participate, which also increases the likelihood of the over-speed incidents.

Based on the simplified governor model in [12], the ‘available PFR’ that can respond within a specified time is expressed as a function of system inertia level when dead band frequency and generation unit are determined. And rather than specifying governor ramp rate directly as in [12], an effective value of available PFR can be introduced into the model to represent the constant linkage between system inertia level and PFR.

## 6.1 CONSTRAINTS CONSIDERING AVAILABLE PFR

Following the discussions above, the “available PFR” will be defined to be the fraction of the headroom that can be utilized to prevent system frequency nadir dropping below the threshold. The available PFR is a function of system inertia level. It is worth to notice that this constraint is still a modification of the co-optimization model, and the minimum requirement on reserve still corresponds to the “worst-case scenario” in ERCOT, which is that when losing two of the largest generation units, the system frequency should be arrested before triggering the UFLS and frequency nadir should be maintained above 59.3Hz. The dynamic simulation results from [6] can still be utilized to generate the modification.

In order to modify the whole model, PFR in previous model needs to be redefined with the concept of “available PFR”. As well as including the tighter constraint on PFR, headroom also needs to be introduced into the model as a variable HR. So that,

$$PFR_{i,t} \leq c_i \cdot (\sum_{i \in G} I_{i,t} \cdot H_i \cdot S_i) \cdot HR_{i,t} \quad \forall i \in G, \forall t \in T \quad (39)$$

In order to interpret the constant  $c_i$ , a value obtained from a macroscopic view, the results of dynamic simulation should be considered. In Table 1, the product of the equivalence ratio and system inertia is about a constant value 260 for the cases with equivalence ratio significantly above 1. Interpreting this observation in the light of the discussion in Chapter 5, if only a fraction of headroom is considered to be available as PFR, then the appropriate fraction is the inertia multiplied by 1/260. So that the newly introduced constraint on available PFR could be

$$0 \leq PFR_{i,t} \leq 1/260 \cdot (\sum_{i \in G} I_{k,t} \cdot H_k \cdot S_k) \cdot HR_{i,t} \quad \forall i \in G, \forall k \in G, \forall t \in T \quad (40)$$

However, due to the product of binary variable and continuous variable, headroom and system inertia, in the constraint above, the optimization model cannot be solved directly. So here the big M method is introduced again to separate the product by relaxing the feasible region, as in [7]. The same method is applied here and (40) is reconstructed as (41), (42), and (43). Besides, the constant number 1/260 is substituted as the reciprocal of equivalency ratio  $\alpha$ . The  $1/260 \cdot (\sum_{i \in G} I_{i,t} \cdot H_i \cdot S_i) \cdot HR_i$  is reconstructed as  $1/Ratio_s$ , since the constant 1/260 is approximated as the product of inertia and equivalency ratio. Following the identical method in [7], the binary variable  $\delta$  is mentioned again to obtain the equivalency ratio  $\alpha$ , which matches the system inertia level.

$$0 \leq PFR_{i,t} \leq \omega_t \quad \forall i \in G, \forall t \in T \quad (41)$$

$$\omega_t \leq \frac{HR_{i,t}}{Ratio_s} - N_{s,t} \cdot (1 - \delta_{s,t} + \delta_{s+1,t}) \quad \forall s \in N, \forall t \in T \quad (42)$$

$$\omega_t \geq \frac{HR_{i,t}}{Ratio_s} + N_{s,t} \cdot (1 - \delta_{s,t} + \delta_{s+1,t}) \quad \forall s \in N, \forall t \in T \quad (43)$$

This formulation takes full advantage of the existing piece-wise/step-wise formulation for requirement on FRR and equivalency ratio  $\alpha$ . Moreover, it converts the constant number  $c_i$  from (39) to the reciprocal of equivalency ratio  $\alpha$ , which has been existing in the original model and avoids introducing another number and further, saves computational effort. The variable  $\omega$  is introduced to relax the feasible region again. Following the big M method, N is a constant number, and the value of it needs to be large enough to cover all the possible values for a single PFR. The preferred value of N should be the largest possible value of HR, which is the highest sustainable limit (HSL) of each generation unit, multiplied with  $(\sum_{i \in G} H_i \cdot S_i)$ . So  $N_{s,t} = HSL_i \cdot (\sum_{i \in G} H_i \cdot S_i)$ . This formulation is named as equivalency ratio modified model (ERMM).

However, the formulations above may not depict equation (40) accurately enough. Although the combination (41), (42), and (43) makes use of the functional linear expression related to binary variable  $\delta$  under the guidance of big M method, introducing the reciprocal of equivalency ratio  $\alpha$  into the formulation is neither necessary nor accurate, because the system inertia value divided by the constant number 260 may not be exact value of equivalency ratio  $\alpha$ . Therefore formulation (40) could be reestablished as (45) and (46), which is named the direct modified model (DMM).

$$PFR_{i,t} \leq 1/260 \cdot HR_{i,t} \cdot (\sum_{k \in G} H_k \cdot S_k) \quad \forall i \in G, \forall k \in G, \forall t \in T \quad (44)$$

$$0 \leq PFR_{i,t} \leq N_i \cdot I_{k,t} \quad \forall i \in G, \forall k \in G, \forall t \in T \quad (45)$$

With further interpretation of DMM mentioned above, however, this kind of formulation is still problematic. This is because formulation (44) and (45) did not consider the commitment of each generation unit is independent, and they did not

separate all generation units and bind them individually. Therefore a new continuous variable  $sPFR$  is introduced to represent the shares in  $PFR$  and assist the model for big M method application. The re-formulation is named as detailed direct modified model (DDMM) and the formulations are shown as:

$$0 \leq sPFR_{i,k,t} \leq HR_{i,t} \cdot (\sum_{k \in G} H_k \cdot S_k) / 260 \quad \forall i \in G, \forall k \in G, \forall t \in T \quad (46)$$

$$sPFR_{i,k,t} \leq N_{i,k} \cdot I_{k,t} \quad \forall i \in G, \forall k \in G, \forall t \in T \quad (47)$$

$$PFR_{i,t} \leq \sum_k sPFR_{i,k,t} \quad \forall i \in G, \forall k \in G, \forall t \in T \quad (48)$$

The constraint (12) related to PFR and HR is also substituted as (49), which is shown below:

$$P_{i,t} + RUP_{i,t} + PFR_{i,t} + HR_{i,t} = HSL_i \cdot I_{i,t} \quad \forall i \in G, \forall t \in T \quad (49)$$

## Chapter 7. Case Study

### 7.1 CASE INTRODUCTION

The computational study is identical to the three wind penetration cases developed in [7], which is based on a modified IEEE-118 bus system with the same topology and enlarged capacity on the same transmission lines, generator units and load level, as shown in Figure 7. The total thermal units capacity is scaled up to 60,000 MW to simulate the situation in ERCOT. In order to simulate the changes of system inertia level, wind power penetration is introduced for interpreting renewable energy influence on the optimization problem considering generation and reserve schedule. Totally six wind farms are added to buses 11,15, 54, 59, 80 and 90, and all the wind farms are identical. It is assumed that the offer price for wind power is \$0.01/MWh. The capacity limits for regulation up reserve, regulation down reserve and PFR from generation units are set as 5%, 5% and 20% of the highest sustainable limits. The offer prices for the regulation up reserve, the regulation down reserve, the non-spinning reserve and PFR are set as 33.3%, 33.3%, 10% and 20% of the prices of their first energy offer segment. All the requirements on reserves are from ERCOT criteria. The regulation up reserve, regulation down reserve, non-spinning reserve requirements are set as the date for March 2017 and can be found in the public page of ERCOT.

To simplify the case study, only three load resources participate in the day-ahead market. The peak capacity limits of the three load resources is listed in Table 2, which are at hour 19, as well as the load energy bid prices and FFR offer prices. The load is modeled as being price elastic load with varied maximum power consumption limit, and all the variations of load level with different hours are shown in Table 3.

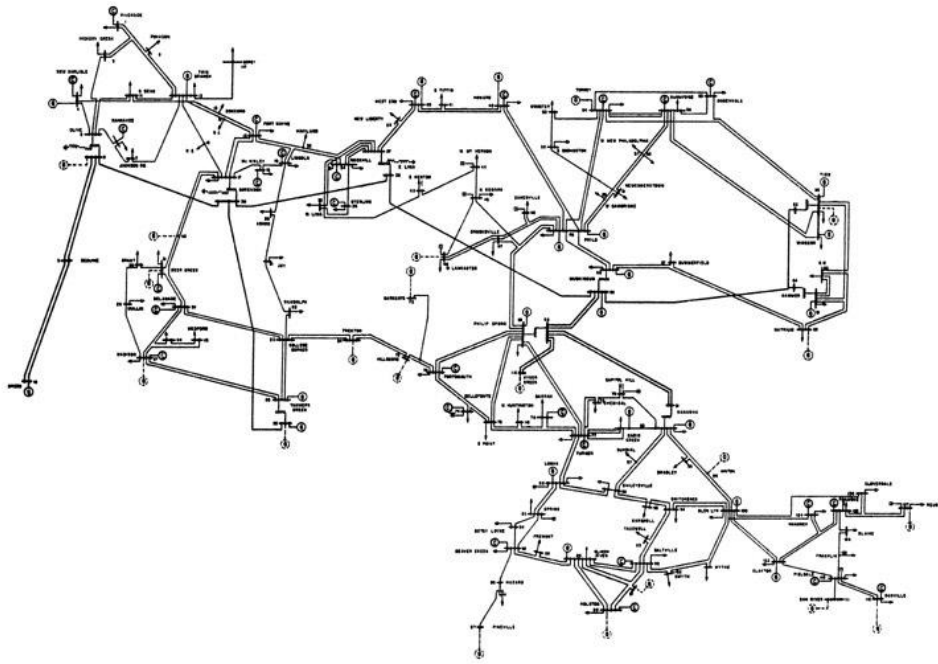


Figure 7: IEEE 118 Bus System Diagram

HOUR 19 (PEAK)	LOAD CAPACITY (MW)	LOAD BIG (\$/MW)	FFR OFFER (\$/MW)
L1	29406	90	45
L2	8822	35	5
L3	2941	6	3

Table 2: Bidding Parameters and Capacities of Load Resources [7] (Source: Table II)

Hour	Capacity Percentage(%)	Hour	Capacity Percentage(%)	Hour	Capacity Percentage(%)
1	79	9	76	17	86
2	75	10	79	18	99
3	72	11	81	19	100
4	71	12	83	20	98
5	71	13	84	21	96
6	72	14	84	22	92
7	74	15	83	23	86
8	75	16	82	24	80

Table 3: Capacity Percentages of Load Resources [7] (Source: Table III)

## 7.2 SCENARIO DESCRIPTION

There are three scenarios simulated in the case study, in order to consider the influence of both renewable generation and FFR price variation, which are described below.

Case A- Low penetration of wind generation and low offer price of FFR. The peak wind power generation in Case A is 3598 MW at hour 4, as shown in Table 4. The FFR offers of the load resources are shown in Table 2.

Case B- High penetration of wind generation and low offer price of FFR. The peak wind power generation in Case B is 14391 MW at hour 4, as shown in Table 5. The FFR offers of the load resources is the same as the FFR offer listed in Table 2.

Case C- High penetration of wind generation and High offer price of FFR. The peak wind power generation in Case C is identical to the wind power in Case B. However, the FFR offers of the load resources 2 is increased to \$10/MWh.

Hour	Wind HSL	Hour	Wind HSL	Hour	Wind HSL
1	3246	9	1764	17	1454
2	3587	10	1655	18	1852
3	3530	11	1243	19	2239
4	3598	12	1261	20	2689
5	3037	13	923	21	2903
6	2631	14	611	22	3177
7	2230	15	1020	23	3283
8	2201	16	1056	24	3319

Table 4: Total High Sustainable Limits of Low Penetration of Wind Generation [7]  
(Source: Table IV)

Hour	Wind HSL	Hour	Wind HSL	Hour	Wind HSL
1	12985	9	10584	17	12792
2	14347	10	11370	18	13548
3	14121	11	12078	19	12534
4	14391	12	12228	20	11184
5	12148	13	12870	21	11610
6	10524	14	11868	22	12709
7	11016	15	11370	23	13132
8	11523	16	12036	24	13275

Table 5: Total High Sustainable Limits of High Penetration of Wind Generation [7]  
(Source: Table V)

### 7.3 OBJECTIVE FUNCTION VALUE

The case study is implemented in Matlab R2018b and solved with gurobi. The results are presented for the four models, including the base model described in [7], the Equivalency Ratio modified model, the direct modified model, and the detailed direct modified model. The results of objective function for base model, ER modified model, direct modified model, and detailed modified model, which is social welfare, are listed in Table 6.

Social Welfare (\$)	Case A	Case B	Case C
Base Model	45378657.80	50218472.72	50177427.09
ER Modified Model	45381386.19	50220019.31	50185799.57
Result Gap1(%)	0.00601	0.00308	0.16686
Direct Modified Model	45381985.16	50220657.26	5029398.06
Result Gap2(%)	0.00811	0.00350	0.20025
Detailed Direct Modified Model	45386987.78	50240988.26	50421760.18
Result Gap3(%)	0.00409	0.04108	0.48556

Table 6: Objective Value

The base model results follow the result from [7], which are \$45,378,657.80 for Case A, \$50,218,472.72 for Case B, and \$50,177,427.09 for Case C, respectively. The difference between objective values is due to more wind power generation in Case B and Case C, substituting part of the thermal generation units and enlarging the social welfare

with lower energy cost. The social welfare results for ER modified model are quite similar to those in base model, which are \$45,381,386.19 for Case A, \$50,220,019.31 for Case B, and \$50,185,799.57 for Case C. The social welfare results for direct modified model are nearly identical to those values for base model, which are \$45,381,864.16 for Case A, \$50,220,231.26 for Case B and \$50,292,957.06 for Case C. The social welfare results for detailed direct modified model are \$45386866.78 for Case A, \$50,240,628.26 for Case B, \$45381864.16 for Case C, which are also close to the base model results.

The gaps between base model and three kinds of modified models are also listed in Table 6 as result gap. The result gaps 1 for ER modified model are 0.00601%, 0.00308% and 0.16686%, respectively. The result gaps 2 for direct modified cases are 0.00705%, 0.00350% and 0.23024%, respectively. The result gaps 3 for detailed direct modified cases are 0.00395%, 0.04103% and 0.48535%, respectively. For all types of the modified models, the final values of objective are highly consistent with the objective values in base model with just tiny amounts of difference. Besides, the results for ER modified cases have a smaller gap compared with those for direct modified cases and thus, are closer to the base objective values, while the detailed direct modified model performs the worst in the three modified models with the largest values in the gap.

For the computational effort comparison, due to the enormous time consumed under the slow solver gurobi, another approach is applied in this report: by limiting the computational time to an identical value for all types of models, the computational gap between the best objective and best bound can be compared for a fixed total

computational effort for each model. A smaller computational gap represents less computational effort needed to solve cases.

Table 7 shows the computational gaps for the base model, ER modified model, direct modified model and detailed direct modified model when the maximum computational time is limited to 600 seconds. Obviously, direct modified cases have similar performance as base cases, while ER modified cases consume more time to solve the problem. This is because compared with direct modified model, ER modified model holds one more constraint, although the variables are identical with the direct modified model. Therefore ER modified model consumes more effort for computation.

The detailed direct modified model performs good in Case C, while not in in Case A and Case B. However, one thing that is worth to notice is that in the detailed direct modified model, a three-dimensional variable  $sPFR$  is included, which consumes quite a long time for the solver to process it. Further consideration may put effort on the model optimization in order to accelerate the rate of data processing.

Computational Gap (%)	Case A	Case B	Case C
Base Model	0.3451	0.3763	0.4013
ER Modified Model	0.4657	0.4650	0.8580
Direct Modified Model	0.3728	0.3789	0.3929
Detailed Direct Modified Model	0.3956	0.3912	0.3328

Table 7: Computational Gap

#### 7.4 DISPATCH RESULTS ANALYSIS

The comparisons of PFR and FFR dispatches for ER modified model and base model are shown in Figure 7 and Figure 8. Both PFR and FFR dispatch are identical in Case A, which means the ER modified definition 'available PFR' has no impact when it is low wind generation and low FFR price case. For Case B, it holds the same amount of PFR for both base case and ER modified case. However, cleared FFR is decreased in the modified case. It is due to the tighter constraint on PFR, which tends to encourage more generators to be turned on in order to fulfill the requirement on PFR. And system inertia level is also increased, leading to a bigger value of equivalent ratio  $\alpha$ . Therefore the amount of FFR is lower in modified Case B. For Case C, the base case tends to procure FFR because of higher price for FFR. However, fulfilling the requirement on frequency response requirement merely by procurement of PFR no longer works under a tighter constraint on PFR. While the price for FFR is increased, turning generation units on to obtain PFR costs even more. Therefore in modified Case C, some amount of FFR is procured to reach the welfare-maximized goal.

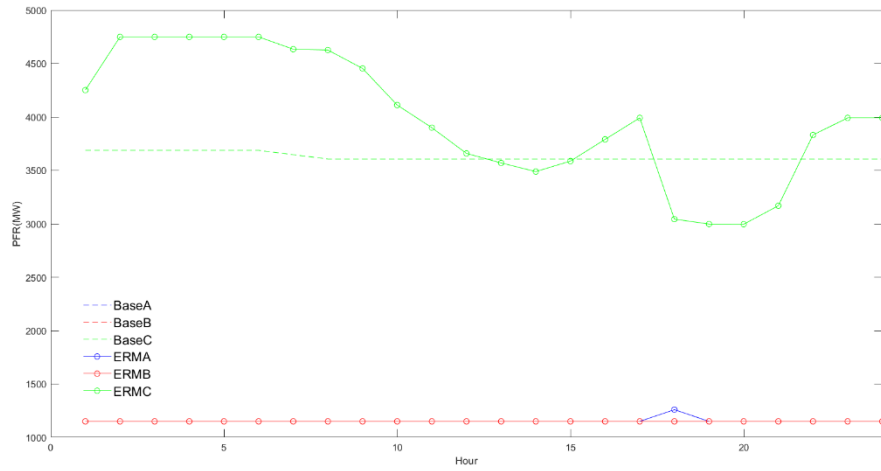


Figure 8: PFR Dispatch Result Comparison: ERMM

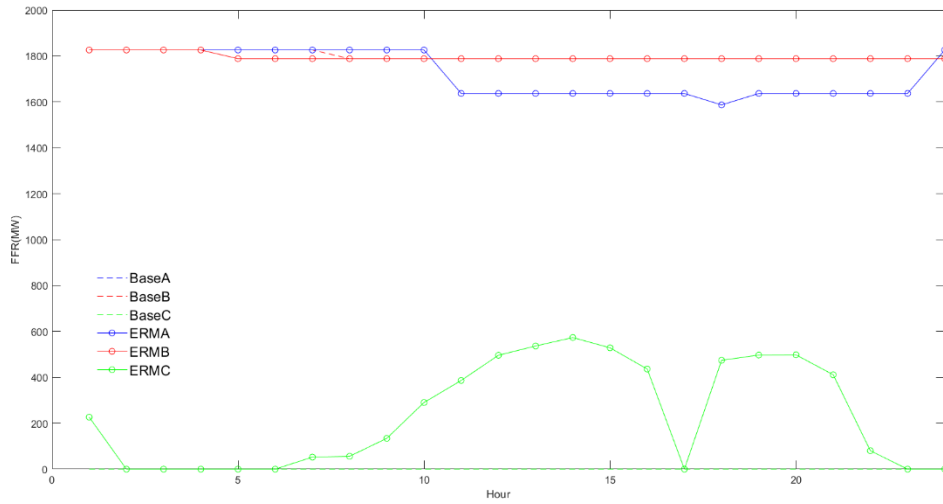


Figure 9: FFR Dispatch Result Comparison: ERMM

The comparisons of PFR and FFR dispatches for direct modified model and base model are shown in Figure 9 and Figure 10. The situations for PFR and FFR dispatch are identical to that in ER modified model, which is the same as base model in Case A and

slight difference from base model in Case B. However, the dispatch in Case C is quite different in the direct modified model compared with ER modified model, and holds a dispatch result more like that in base model with inconsistency in hour 17 to hour 21. This is due to the new constraint on PFR, which limits the amount of PFR that can be provided by operating generation units and tends to encourage load resource offers some amount of FFR to fulfill the requirement of frequency reserve after comparing the cost to turn on extra generators and maintain them operating and the cost to procure FFR, even though the price for FFR is much higher than that for PFR.

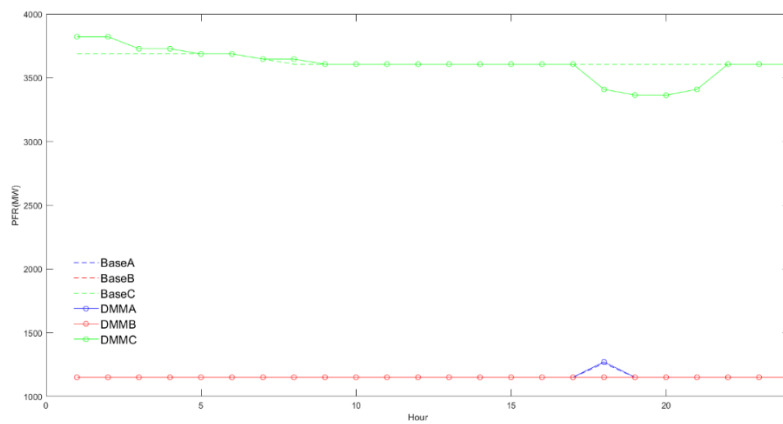


Figure 10: PFR Dispatch Result Comparison: DMM

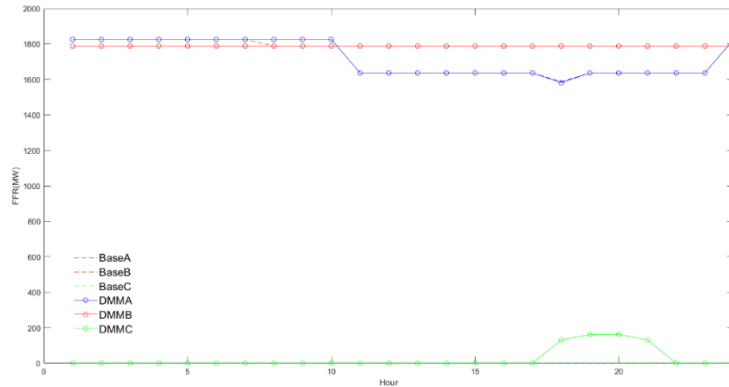


Figure 11: FFR Dispatch Result Comparison: DMM

The comparisons of PFR and FFR dispatches for detailed direct modified model and base model are shown in Figure 11 and Figure 12. The dispatch result of PFR is identical in Case A and Case B, compared with the base model results. For result in Case C, although there is slight difference in the PFR dispatch in the few hours at the beginning, the trend is quite similar to the result from base model, which performs better than both the ER model and the DM model. For the dispatch results of FFR, it is basically the same as those in the base model, only with slight difference for Case A and Case B, in hour 6 and hour 24 respectively. Compared with the results in direct modified model, detailed direct modified model performs well in Case C and does not dispatch any FFR during the whole 24 hours, which is consisted with base model. So detailed direct modified model holds the correct formulation, although with far more complicated constraints.

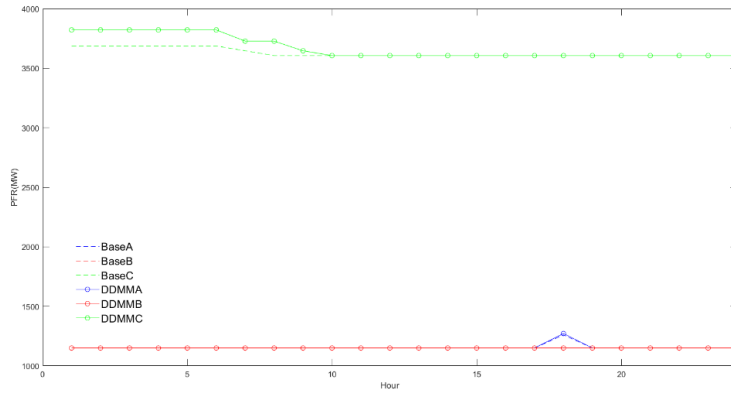


Figure 12: PFR Dispatch Result Comparison: DDMM

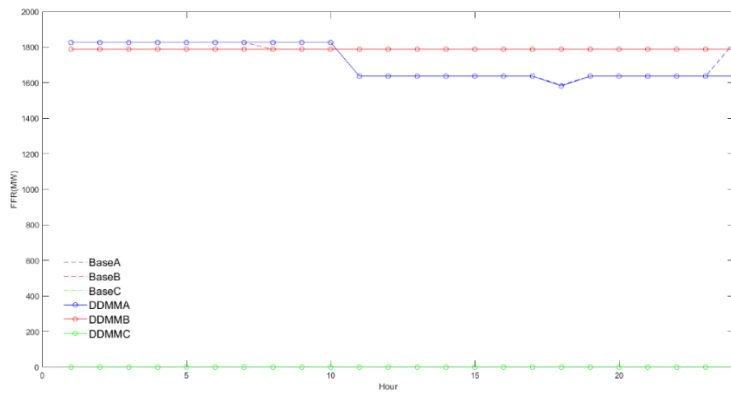


Figure 13: FFR Dispatch Result Comparison: DDMM

### 7.5 CLEARED PRICES COMPARISON

The cleared price for day-ahead market are from the Lagrange multipliers of corresponding binding constraints. In the co-optimization model, which is a mixed integer nonlinear programming model, the Lagrange multipliers correspond to the constraints in the linear model with all the binary variables fixed at the committed results.

The dual variables  $\lambda$ ,  $\theta$ ,  $\gamma$ ,  $\rho$ ,  $\tau$ ,  $\pi$ ,  $\sigma$  are the Lagrange multipliers corresponding to the constraints (20)-(26) in the co-optimization model in Chapter 4. The marginal price for

energy is calculated by  $\lambda_t - \sum_{l \in B} SF_l \cdot \theta_l$ . The prices for regulation up reserve, regulation down reserve, and non-spinning reserves are  $\gamma$ ,  $\rho$  and  $\sigma$  respectively.

The marginal price for PFR is  $\pi$  for meeting the minimum PFR requirement, which is constraint (25), and  $\sigma$  for meeting the minimum FRR requirements, which is constraint (26), so the price for PFR is  $\pi + \sigma$ , since both of the constraints limit PFR. If the thermal generation units are the marginal resources to supply FRR, the cleared price for PFR at a particular hour will reflect the PFR offer. The FFR price is  $\alpha_t + \sigma$  to account for the equivalency ratio between the FFR and PFR. If the load resource is the marginal resource for FRR, both PFR offer and FFR offer will influence the PFR since the minimum requirement on PFR constraint is binding. The cleared price for FFR is based on the FRR marginal price and the equivalency ratio  $\alpha$  if the generation units is marginal when providing FRR. However, if load resource provides FRR, the offer price from FFR determines the FFR cleared price.

As shown above, the cleared prices for PFR and FFR from the base model, the ER modified model, the DM model and DDM model are discussed as follows.

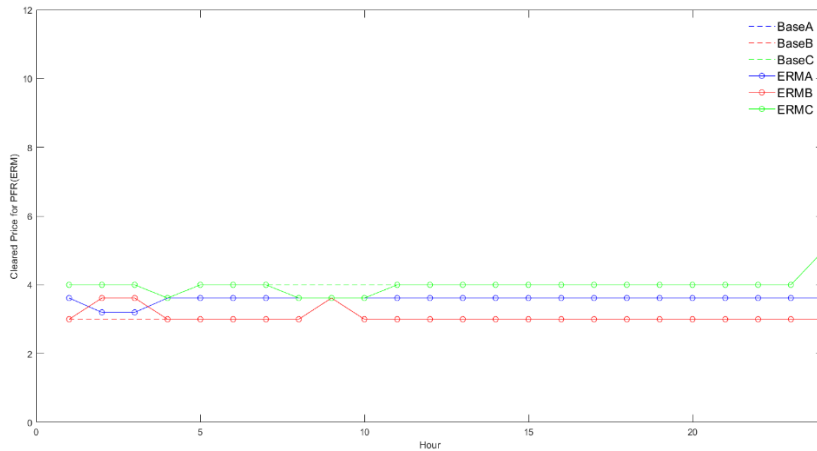


Figure 14: Cleared price comparison for PFR: ERMM

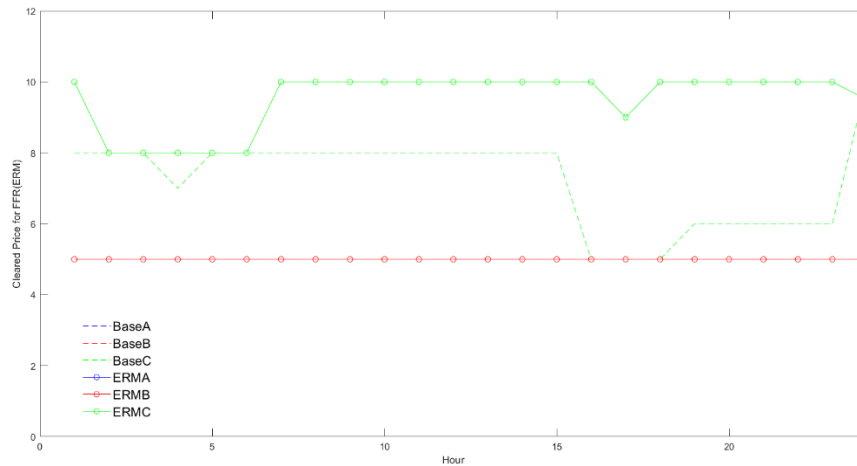


Figure 15: Cleared price comparison for FFR: ERMM

The cleared prices for PFR and FFR for both the base model and ER modified model are shown in Figure 13 and Figure 14. The PFR and FFR cleared prices are quite similar to those in base model in Case A and B. It is because the dispatch in ER modified model is identical, which means the marginal generation units in base model and marginal FFR resource from L2 are still the same as those in ER modified model in Case A and B. However, for Case C, some amount of FFR is still procured from load resource even under the high offer price, which is because procurement of PFR needs to turn on and keep on more thermal generators, which cost even more. Therefore the cleared prices for FFR raise up to \$10, which is the offer price for FFR for some hours.

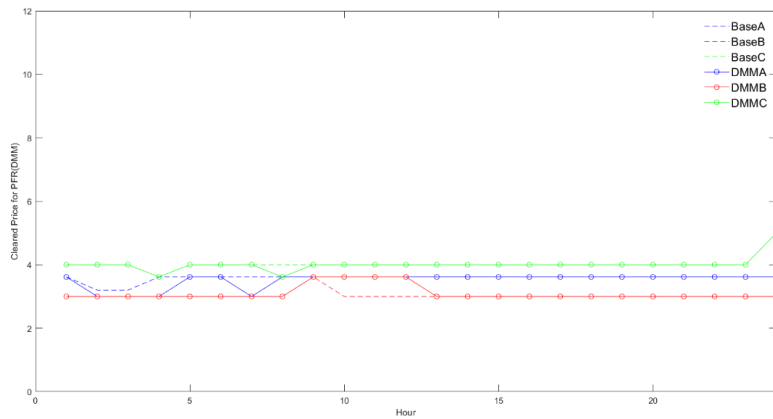


Figure 16: Cleared price comparison for PFR: DMM

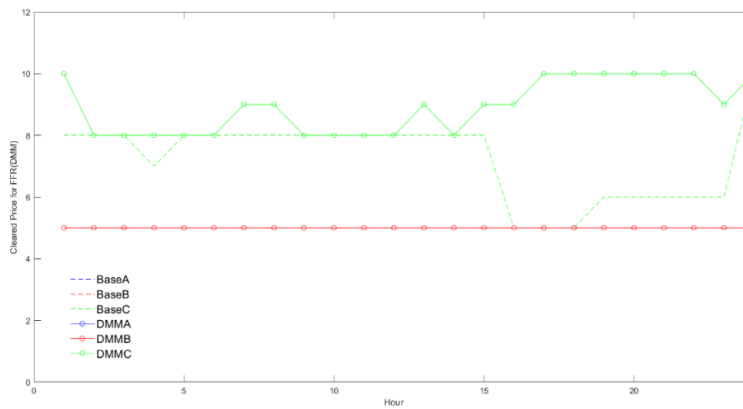


Figure 17: Cleared price comparison for FFR: DMM

The cleared prices for PFR and FFR for both the base model and ER modified model are shown in Figure 13 and Figure 14. The PFR and FFR cleared prices are quite similar to those in base model in Case A and B. It is because the dispatch in ER modified model is identical, which means the marginal generation units in base model and marginal FFR resource from L2 are still the same as those in ER modified model in Case A and B. However, for Case C, some amount of FFR is still procured from load resource even under

the high offer price, which is because procurement of PFR needs to turn on and keep on more thermal generators, which cost even more. Therefore the cleared prices for FFR raise up to \$10, which is the offer price for FFR for some hours.

For the cleared PFR and FFR prices for direct modified model, the price for PFR is basically the same as those in base model for Case A and Case B, which are shown in Figure 15 and Figure 16, since the cases have the same dispatch results and the same marginal providers. And for Case C, the dispatch result in direct modified model is closer to that in base model with only 4-hour difference in FFR procurement. The difference in results is again due to a relatively higher cost to continue to obtain PFR from generation units and turn them on. The cleared price for FFR can reach \$10 when FFR is considered to fulfill the requirement on FRR.

For the cleared PFR and FFR prices for detailed direct modified model, the price for PFR is basically the same as those in base model for Case A and Case B too, which are shown in Figure 17 and Figure 18. However, there is small difference in a few beginning hours and ending hours. This is due to the slight dispatch difference due to the tighter PFR constraint, which causes the difference of marginal generation units. For Case C, the cleared prices for FFR deviate from the results in base model. It is due to the variation on constraint (25), which leads to the different values of the Lagrange multiplier  $\pi$ , and causes the cleared price deviation, although the FFR dispatch result is the same as that in base model.

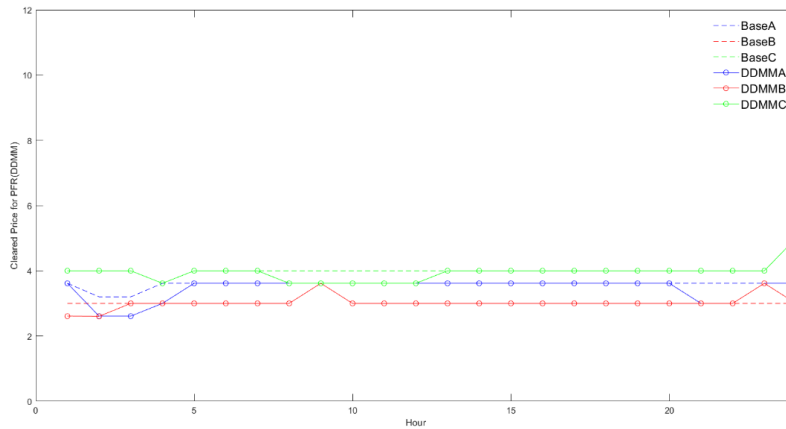


Figure 18: Cleared price comparison for PFR: DDMM

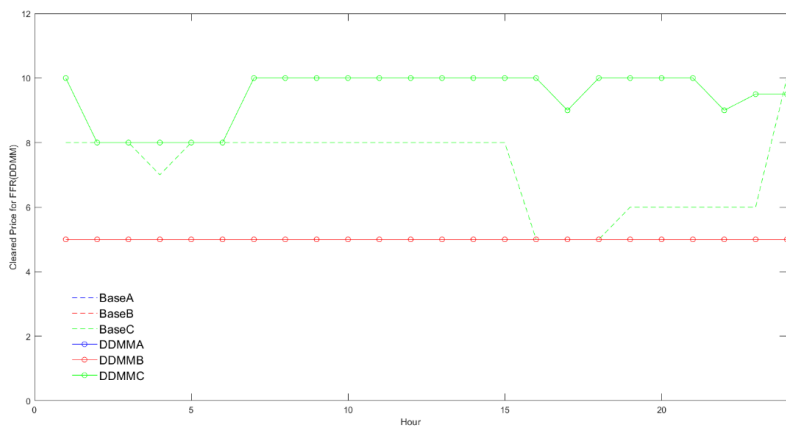


Figure 19: Cleared price comparison for FFR: DDMM

It is worth to note that the cleared prices mentioned in the co-optimization model are all offer prices or bid prices, which means these prices are the values submitted to the Independent System Operators (ISOs) in the day-ahead market, and used for scheduling for next day. However, these are not the same as the final cleared prices on the day-ahead market if the corresponding offer or bid is not marginal. The co-optimization model

mentioned above follows the ERCOT criteria, where the offers from participants are included in the objective function as cost.

However, following [15], the ISO-NE chooses to include zero reserve prices in the objective function. If such formulation is introduced into this co-optimization model, the ISO would tend to procure FFR as much as possible to fulfill the requirement on FRR because of its effectiveness, while the amount of PFR would just be the minimum requirement on itself.

## Chapter 8. Conclusion

This report is based on the model from [7], which discussed procurement of reserve to maintain system frequency from both load resources and generation units within market frame and requirements on interaction of PFR and FFR. However, further discussion introduces the concept of headroom and governor model, which leads to a description including the governor ramp rate. Therefore the modified concept 'available PFR' is presented as a fraction of headroom, representing the part of non-dispatched capacity that can be utilized before the system frequency nadir. The modified “available PFR” is also a function of system inertia level, and the constant coefficient  $c_i$  is obtained from dynamic simulations. As a result, this alternative constraint is added into the co-optimization model to substitute former PFR, along with headroom as a variable.

In order to separate the two multiplied variables and allow the added constraint to coordinate with mix integer solver gurobi, the same linear formation technique with big M method is proposed again as in [7]. The same three scenarios are introduced into the case study and are compared with results from base model in [7]. The results show the effectiveness of the alternative formulation of PFR.

Although this work just discusses a potential direction of modification of co-optimization model considering both power and reserve simultaneously, the train of thought can be applied to other factors of such model, which can be revised in detail and finally holds more accurate descriptions of constraints, such as dynamics of load variations and system inertia level.

## Chapter 9. Future Work

Except for the interpretation on details from governor response modeling, works related to the coordination and contribution from all kinds of frequency response contributors are also worth discussing. Based on the four contributors to restoring supply-demand curve listed in [16], including synchronous inertia, governor response, FFR and under-frequency load shedding, the response rate of each type of contributors becomes critical, due to the penetration of renewable generation resources, causing the decline in system inertia level and the increase on the rate of change of frequency (RoCoF). Therefore the low-inertia system is ‘lighter’ compared with high-inertia system. In order to interpret the contribution provide from each contributor, dynamic simulations are made in [16], which is quite similar to the approach in [6].

With the increase in the RoCoF, the requirement on frequency response has two aspects: response rate and response duration. Since the goal of frequency response is to arrest the frequency drop and prevent frequency dropping below the threshold for UFLS, fast frequency response occupies a more significant role because of the 30-cycle dispatch dead band, which is far better compared to traditional governor response. Besides, response duration represents the amount of energy injected into the system during frequency deviation, which means more FFR is needed to substitute the governor response and fulfill the requirement on frequency response. In addition, increasing amount of FFR can also bring the frequency nadir up with the decline of system inertia.

System inertia is the first response to the imbalance of power system. Therefore the inertia-FFR relationship is worth to interpret in the low-inertia system. A different ‘equivalency ratio’ is introduced in [17] to show the inertia-FFR relationship, which offers a clear view on the trade-off when thermal generation units are substituted with renewable

resources and on the amount of FFR needed to fulfill the requirement on frequency response.

Other potential research directions may include the policies and mechanisms encouraging the load resource to participate in the electricity market to provide the FFR needed in the system, as well as the location choices of FFR resource, which is not coordinated within the day-ahead market scheduling process. After all, coordination of all available resources must be taken into consideration to ensure grid stability.

## Bibliography

- [1] Rebours, Yann G., et al. "A survey of frequency and voltage control ancillary services—Part I: Technical features." *IEEE Transactions on power systems* 22.1 (2007): 350-357.
- [2] Rebours, Yann G., et al. "A survey of frequency and voltage control ancillary services—Part II: Economic features." *IEEE Transactions on power systems* 22.1 (2007): 358-366.
- [3] G. Delille, B. Francois, and G. Malarange, "Dynamic frequency control support by energy storage to reduce the impact of wind and solar generation on isolated power system's inertia," *IEEE Trans. Sustain. Energy*, vol. 3, no. 4, pp. 931–939, Oct. 2012.
- [4] Energy Regul. Comm., Third-Party Provision of Primary Frequency Response Service, Fed, Washington, DC, USA, Nov. 20, 2015.
- [5] NERC Reliability Standard BAL-003 Frequency Response and Frequency Bias Setting, NERC.
- [6] W. Li, P. Du, N. Lu, "Design of a new primary frequency control market for hosting frequency response reserve offers from both generators and loads," *IEEE Transactions on Smart Grid*, 2017 Feb 23.
- [7] Liu, Cong, and Pengwei Du. "Participation of load resources in day-ahead market to provide primary-frequency response reserve." *IEEE Transactions on Power Systems* 33.5 (2018): 5041-5051.
- [8] Baldick, Ross. *Applied optimization: formulation and algorithms for engineering systems*. Cambridge University Press, 2006.
- [9] L. Fan, J. Wang, R. Jiang, Y. Guan, "Min-max regret bidding strategy for thermal generator considering price uncertainty," *IEEE Transactions on Power Systems*. Vol. 29, No. 5, pp. 2169-2179, 2014.
- [10] P. Kundur, *Power system Stability and Control*. New York, NY, USA: McGraw-Hill, 1994, p. 584.
- [11] Power World Governor Block Diagrams [Online].

- [12] Chávez, Héctor, Ross Baldick, and Sandip Sharma. "Governor rate-constrained OPF for primary frequency control adequacy." *IEEE Transactions on Power Systems* 29.3 (2014): 1473-1480.
- [13] Ross Baldick, and Sandip Sharma. "Governor rate-constrained OPF for primary frequency control adequacy." *IEEE Transactions on Power Systems* 29.3 (2014): 1473-1480.
- [14] ERCOT Nodal Operating Guides, Section 8, Attachment C: Turbine Governor Speed Tests [Online]. Available: <http://www.ercot.com/content/mktrules/guides/noperating/current/08C-TurbineGovernor-SpeedTests-010112.doc>
- [15] Zheng, Tongxin, and Eugene Litvinov. "Contingency-based zonal reserve modeling and pricing in a co-optimized energy and reserve market." *IEEE transactions on Power Systems* 23.2 (2008): 277-286.
- [16] D. Stenlik, M. Richwine, N. Miller, L. Hong. " The Role of Fast Frequency Response in Low Inertia Power Systems" CIGRE 2018. 2018.
- [17] Miller, N.; Clark, K.; Walling, R., "WindINERTIA: Controlled Inertial Response from GE Wind Turbine Generators." Presented at the 45th Annual Minnesota Power Systems Conference, Minneapolis, Minnesota, November, 2009.
- [18] R. Baldick, "Wind and energy markets: A case study of Texas," *IEEE Syst. J.*, vol. 6, no. 1, pp. 27–34, Mar. 2012.
- [19] S. Stoft, *Power System Economics: Designing Markets for Electricity*. Piscataway, NJ, USA: IEEE Press/Wiley Interscience, 2002.
- [20] Sharma, Sandip, Shun-Hsien Huang, and N. D. R. Sarma. "System inertial frequency response estimation and impact of renewable resources in ERCOT interconnection." 2011 IEEE power and energy society general meeting. IEEE, 2011.